AIMS Mathematics, 9(7): 17339–17358.
DOI: 10.3934/math.2024843
Received: 05 February 2024
Revised: 19 April 2024
Accepted: 26 April 2024
Published: 20 May 2024

https://www.aimspress.com/journal/Math

Research article

Numerical investigation of nonlinear extended Fisher-Kolmogorov equation via quintic trigonometric B-spline collocation technique

Shafeeq Rahman Thottoli[1], **Mohammad Tamsir**[2], **Mutum Zico Meetei**[2,*] **and Ahmed H. Msmali**[2,3]

[1] Department of Physical Sciences, Physics Division, College of Science, Jazan University, P.O. Box 114, Jazan 45142, Kingdom of Saudi Arabia

[2] Department of Mathematics, College of Science, Jazan University, P.O. Box 114, Jazan 45142, Kingdom of Saudi Arabia

[3] School of Mathematics and Applied Statistics, University of Wollongong, Wollongong, NSW 2522, Australia

* **Correspondence:** Email: mmeetei@jazanu.edu.sa.

Abstract: In this article, a collocation technique based on quintic trigonometric B-spline (QTB-spline) functions was presented for homogeneous as well as the nonhomogeneous extended Fisher-Kolmogorov (F-K) equation. This technique was used for space integration, while the time-derivative was discretized by the usual finite difference method (FDM). To handle the nonlinear term, the process of Rubin-Graves (R-G) type linearization was employed. Three examples of the homogeneous extended F-K equation and one example of the nonhomogeneous extended F-K equation were considered for the analysis. Stability analysis and numerical convergence were also discussed. It was found that the discretized system of the extended F-K equation was unconditionally stable, and the projected technique was second order accurate in space. The consequences were portrayed graphically to verify the accuracy of the outcomes and performance of the projected technique, and a relative investigation was accomplished graphically. The figured results were found to be extremely similar to the existing results.

Keywords: homogeneous and nonhomogeneous extended F-K equation; collocation technique; QTB-spline functions; R-G type linearization process; stability analysis; convergence
Mathematics Subject Classification: 35-XX, 65-XX, 74S30

1. Introduction

Nonlinear partial differential equations (PDEs) are extremely significant in real-world applications, which is why they play a significant part in the modeling of natural events. Most real-world problems can be characterized by nonlinear PDEs. However, analytical methods are unable to resolve some of these problems. Several numerical methods have been applied to solve these equations.

The Fisher Kolmogorov (F-K) models have been extensively utilized in the study of physical, material, and biological systems [1]. Some of these applications include, for instance, pattern formation [2], spatiotemperal chaos [3], traveling waves phenomena [4], liquid crystals domain walls propagation [5], reaction model for Alzheimer's disease [6], and tumor growth dynamics [7].

A cubic B-spline differential quadrature technique (DQM) was applied to simulate the fourth-order extended F-K equation in [8]. Error norms were used to assess the accuracy of the method. DQM and discretization were used to solve PDEs in [9]. Authors of [10, 11] utilized differential quadrature and collocation methods based on quintic B-spline (QB) functions, i.e., QBDQM and QBCM, respectively, to simulate a numerically extended F-K (EFK) model. An analysis was conducted on stability, rate of convergence, and error norms. A numerical approach using trigonometric cubic B-spline functions was introduced to solve the time fractional gas dynamics equation was introduced in [12]. The generalized nonlinear time-fractional Klein-Gordon equation (TFKGE) was solved numerically using extended cubic B-spline (ECBS) functions in [13].

In [14], a trigonometric quintic B-spline method is employed to solve singularly perturbed boundary value problems, proving its ease and cost-effectiveness. A recent study used a trigonometric quintic B-spline method to solve the Korteweg-de Vries (KdV)-Kawahar equation, which has time-dependent parameters [15]. The numerical results obtained from this method were shown to be both effective and efficient. The trigonometric cubic and quintic B-splines are utilized to simulate the Burgers equation [16]. The accuracy of the outcome is evaluated by error norms and compared to the available approximate solutions. Results showed that the approach is exceptionally effective in resolving coupled Burgers' equation (cBE). A messless method (finite pointset) was applied in [17], to numerically solve the EFK equation. In [18], mesh-free numerical techniques were used based on DQM and radial basis functions (RBF) to simulate the F-K extended model. In [19], the authors used the Fourier-based meshless approach to solve a (3+1)-dimensional PDE. In [20], a Gaussian-cubic backward substitution method was utilized to solve nonlinear and linear problems in two dimensions and three dimensions with an irregular domain. The method's computational accuracy was effectively demonstrated.

The authors of [21] adopted element-free Galerkin interpolation to solve EFK numerically. In [22], the study on stochastic EFK was expanded by employing the numerical technique of Euler-Maruyama. In [23], He's variational method was adopted to study the solitons and period wave solution for EFK. This method simplifies calculation by reducing the order of the equation compared to previous methods. The authors of [24] proposed an approach to solve the EFK problem utilizing 2nd order splitting and orthogonal cubic spline collocation. Applying an H^1-Galerkin mixed finite element (H1-GMFE) method to the extended F-K equation via the splitting method, [25] derived optimal order error estimates. The authors of [26] utilized the C1-conforming finite element method to estimate error optimally for two-dimensional EFK equations (semi and wholly discrete). The authors of [27] analyzed the solution to the EFK equation in terms of its long-term behavior. In [28], the author presented a Crank-Nicolson finite difference scheme (CNFDS) to solve the EFK problem in two space

dimensions with Dirichlet boundary conditions. In [29], the stability of the CNFDS in L_∞ discrete norm for the EFK equation was investigated. The numerial solution to the EFK equation was derived in [30] using quartic B-spline based DQM (QAB-DQM). A novel meshless local collocation approach for numerically solving the 3D extended EFK equation was proposed in [31]. To discretize the time and spatial derivatives of the EFK equation, the second-order Crank-Nicolson scheme and meshless generalized finite difference method (GFDM) were used. Furthermore, in [32], a hybrid numerical method was introduced to address 2D nonlinear transient heat conduction concerns with temperature-dependent conductivity. They used Krylov deferred correction (KDC) for temporal discretization and GFDM for spatial discretization. In light of the aforementioned study, we propose a quintic trigonometric B-spline collocation technique to numerically simulate the extended F-K equation, which is expressed as:

$$u_t + \gamma u_{xxxx} - u_{xx} + u^3 - u = f(x,t), \quad x \in [a,b], t \in [0,T], \tag{1.1}$$

subject to initial condition (IC)

$$u(x,0) = \phi(x), \tag{1.2}$$

and boundary condition (BC)

$$\begin{aligned} u(a,t) &= \psi_1(t), \quad u(b,t) = \psi_2(t), \\ u_{xx}(a,t) &= 0, \quad u_{xx}(b,t) = 0. \end{aligned} \tag{1.3}$$

If $\gamma = 0$ in (1.1), we obtain the standard F-K equation, and its generalization is given as follows:

$$u_t = u_{xx} + u - u^3. \tag{1.4}$$

When approaching Lifshitz points, [33] phase transitions require the inclusion of the fourth-order derivative due to the necessity of including higher-order gradient factors in the energy-free functional. The EFK equation appears at the phase transition Lifshitz point, and the gradient systems evolution equation is given as follows:

$$I(u) = \int \left[\frac{\gamma}{2}(u'')^2 + \frac{\beta}{2}(u')^2 + F(u) \right] dx, \tag{1.5}$$

where F is the double-well potential and is given as follows:

$$F(u) = \frac{1}{4}(1 - u^2)^2. \tag{1.6}$$

If we choose $\beta = 1$, then we obtain the EFK equation.

For the structure of this paper: Section 2 includes the preliminaries about the quadratic trigonometric B-spline (QTB-spline) functions. In Section 3, we present the discretization of the extended F-K equation. Section 4 shows the stability analysis of the discretized system of the F-K equation using the von Neumann method. Section 5 shows the simulation of the F-K equation through numerical examples and compares the accuracy of the results. The conclusions are given in Section 6.

2. QTB-spline basis functions

The problem domain $x \in [a, b]$ is uniformly partitioned into a mesh of length $h = \Delta x = \frac{b-a}{M}$, using the knots $x_i = a + ih$, $i = 0, 1, ..., M$, ensuring that $a = x_0 < x_1 < x_2 < \ldots < x_M = b$. Now, we specify the QTB-spline functions $\hat{Q}_i(x)$ for $i = -2, -1, 0, ..., M+$ as follows:

$$\hat{Q}_i(x) = \frac{1}{\theta}\begin{cases} \rho^5(x_{i-3}), & x \in [x_{i-3}, x_{i-2}), \\ -\rho(x_{i-1})\rho^4(x_{i-3}) - \rho(x_i)\rho(x_{i-2})\rho^3(x_{i-3}) \\ -\rho(x_{i+1})\rho^2(x_{i-3})\rho^2(x_{i-2}) - \\ \rho(x_{i+2})\rho(x_{i-3})\rho^3(x_{i-2}) - \rho^4(x_{i-2})\rho(x_{i-3}), & x \in [x_{i-2}, x_{i-1}), \\ \rho^2(x_i)\rho^3(x_{i-3}) + \rho^2(x_{i-3})[\rho(x_i)\rho(x_{i+1})\rho^2(x_{i-3})\rho(x_{i-2}) \\ +\rho^2(x_{i+1})\rho(x_{i-1})] + \rho(x_{i+2})\ [\rho^2(x_i)\rho(x_{i+2})\rho(x_{i-3})\rho^2(x_{i-2}) \\ +\rho(x_{i+1})\rho(x_{i-3})\rho(x_{i-2})\rho(x_{i-1})] + \\ \rho^2(x_{i+2})\rho(x_{i-3})\rho^2(x_{i-1}) \\ +\rho(x_{i+3})\rho(x_{i+2})\rho(x_{i-2})\rho^2(x_{i-1}) + \rho^3(x_{i-1})\rho^2(x_{i+3}), & x \in [x_{i-1}, x_i), \\ -\rho^3(x_{i+1})\rho^2(x_{i-3}) - \rho(x_{i-3})[\rho(x_{i+2})\rho^2(x_{i+1})\rho(x_{i-3})\rho(x_{i-2}) \\ -\rho^2(x_{i+2})\rho(x_{i+1})\rho(x_{i-1})] - \rho^3(x_{i+2})\rho(x_{i-3})\rho(x_i) \\ -\rho(x_{i+3})[\rho^2(x_{i-1})\rho^2(x_{i-2})\rho(x_{i+3}) + \\ \rho^2(x_{i+1})\rho(x_{i+2})\rho(x_{i-2})\rho(x_{i-1}) \\ +\rho(x_{i-2})\rho^2(x_{i+2})\rho(x_i)] - \rho^2(x_{i+3})[\rho^2(x_{i-1})\rho(x_{i+1}) \\ +\rho(x_{i-1})\rho(x_{i+2})\rho(x_i)] - \rho^3(x_{i+3})\rho^2(x_i), & x \in [x_i, x_{i+1}), \\ \rho^4(x_{i+2})\rho(x_{i-3}) + \rho(x_{i+3})\rho^3(x_{i+2})\rho(x_{i-2}) + \\ \rho^2(x_{i+3})\rho^2(x_{i+2})\rho(x_{i-1}) \\ +\rho(x_i)\rho(x_{i+2})\rho^3(x_{i+3}) + \rho(x_{i+1})\rho^4(x_{i+3}), & x \in [x_{i+1}, x_{i+2}), \\ -\rho^5(x_{i+3}), & x \in [x_{i+2}, x_{i+3}), \\ 0, & \text{otherwise}, \end{cases} \tag{2.1}$$

where $\rho(x_i) = sin(\frac{x-x_i}{2})$, $i = 0, 1, .., M$, and $\theta = sin(2.5h)sin(2h)sin(1.5h)sin(h)sin(0.5h)$.

The QTB-spline functions $\{QT_{-2}, QT_{-1}, ..., QT_{M+1}, QT_{M+2}\}$ form a basis over the problem domain. Table 1 displays QTB-spline values and derivatives at knots.

Table 1. $\hat{Q}_i(x)$ and its derivatives at knots.

x	x_{i-2}	x_{i-1}	x_i	x_{i+1}	x_{i+2}
$\hat{Q}_i(x)$	τ_1	τ_2	τ_3	τ_2	τ_1
$\hat{Q}_i'(x)$	τ_4	τ_5	0	$-\tau_5$	$-\tau_4$
$\hat{Q}_i''(x)$	τ_6	τ_7	τ_8	τ_7	τ_6
$\hat{Q}_i'''(x)$	τ_9	τ_{10}	0	$-\tau_{10}$	$-\tau_9$
$\hat{Q}_i^{iv}(x)$	τ_{11}	τ_{12}	τ_{13}	τ_{12}	τ_{11}

Where

$$\begin{aligned}
\tau_1 &= \frac{1}{\theta}sin^5(\frac{h}{2}), \quad \tau_2 = (2sin^5(\frac{h}{2})cos(\frac{h}{2})(16cos^2(\frac{h}{2}) - 3))/\theta,\\
\tau_3 &= 2(1 + 48cos^4(\frac{h}{2}) - 16cos^2(\frac{h}{2}))sin^5(\frac{h}{2})/\theta, \quad \tau_4 = (-5/2)sin^4(\frac{h}{2})cos(\frac{h}{2})\theta,\\
\tau_5 &= -5sin^4(\frac{h}{2})cos^2(\frac{h}{2})(8cos^2(\frac{h}{2}) - 3)/\theta, \quad \tau_6 = (5/4)sin^3(\frac{h}{2})(5os^2(\frac{h}{2} - 1)/\theta,\\
\tau_7 &= (5/2)sin^3(\frac{h}{2})cos(\frac{h}{2})(-15cos^2(\frac{h}{2}) + 3 + 16cos^4(\frac{h}{2}))/\theta,\\
\tau_8 &= (-5/2)sin^3(\frac{h}{2})(16cos^6(\frac{h}{2} - 5cos^2(\frac{h}{2} + 1)/\theta,\\
\tau_9 &= (-5/8)sin^2(\frac{h}{2})cos(\frac{h}{2})(25cos^2(\frac{h}{2}) - 13)/\theta,\\
\tau_{10} &= (-5/4)sin^2(\frac{h}{2})cos^2(\frac{h}{2})(8scos^4(\frac{h}{2}) - 35cos^2(\frac{h}{2}) + 15)/\theta,\\
\tau_{11} &= (5/16)(125cos^4(\frac{h}{2}) - 114cos^2(\frac{h}{2}) + 13)sin(\frac{h}{2})/\theta,\\
\tau_{12} &= (-5/8)sin(\frac{h}{2})cos(\frac{h}{2})(176cos^6(\frac{h}{2}) - 137cos^7(\frac{h}{2}) - 6cos^2(\frac{h}{2}) + 15)/\theta,\\
\tau_{13} &= (5/8)(92cos^6(\frac{h}{2}) - 117cos^4(\frac{h}{2}) + 62cos^2(\frac{h}{2}) - 13)(-1 + 4cos^2(\frac{h}{2}))sin(\frac{h}{2})/\theta.
\end{aligned}$$

Now, we undertake that the estimation $u_M(x,t)$ to the function $u(x,t)$ at (x,t_j) is represented by:

$$u(x,t) \approx u_M(x,t) = \sum_{i=-2}^{M+2} C_i(t_j)\hat{Q}_i(x), \tag{2.2}$$

where, $C_i(t_j)$ are unknowns and need to be found using the initial and BCs, as well as the collocation technique. Each QTB-spline consists of six components, and each component is included in six QTB-splines. The function $u_M(x,t)$ can be represented as the variation over the component and stated as:

$$u\left(x_M,t_j\right) = \sum_{k=i-2}^{i+2} \hat{Q}_k\left(x\right) C_k\left(t_j\right). \tag{2.3}$$

Using Eq (2.3), u, u_x, u_{xx}, u_{xxx}, and u_{xxxx} the knots can be expressed as:

$$u_i^j = \tau_1 C_{i-2}^j + \tau_2 C_{i-1}^j + \tau_3 C_i^j + \tau_2 C_{i+1}^j + \tau_1 C_{i+2}^j, \tag{2.4}$$

$$(u_x)_i^j = -\tau_4 C_{i-2}^j - \tau_5 C_{i-1}^j + \tau_5 C_{i+1}^j + \tau_4 C_{i+2}^j, \tag{2.5}$$

$$(u_{xx})_i^j = \tau_6 C_{i-2}^j + \tau_7 C_{i-1}^j + \tau_8 C_i^j + \tau_7 C_{i+1}^j + \tau_6 C_{i+2}^j, \tag{2.6}$$

$$(u_{xxx})_i^j = -\tau_9 C_{i-2}^j - \tau_{10} C_{i-1}^j + \tau_{10} C_{i+1}^j + \tau_9 C_{i+2}^j, \tag{2.7}$$

$$(u_{xxxx})_i^j = -\tau_{11} C_{i-2}^j - \tau_{12} C_{i-1}^j + \tau_{13} C_i^j + \tau_{12} C_{i+1}^j + \tau_{11} C_{i+2}, \tag{2.8}$$

where $C_i^j = C_i(t_j)$.

3. The problem's discretization

Currently, the time derivative of the problem (1.1) is discretized by the usual FDM, while θ-weighted scheme is used for spatial derivatives as follows:

$$\frac{u_i^{j+1}-u_i^j}{\Delta t}+\gamma\left[\left(\theta u_{xxxx}\right)_i^{j+1}+(1-\theta)(u_{xxxx})_i^j\right]-\left[\theta(u_{xx})_i^{j+1}+(1-\theta)(u_{xx})_i^j\right]+\theta(u^3)_i^{j+1}$$
$$+(1-\theta)(u^3)_i^j-\theta u_i^{j+1}-(1-\theta)u_i^j=f_i^j. \tag{3.1}$$

The Rubin-Graves [34] approach linearizes the term u^3 as follows:

$$\begin{aligned}(u^3)_i^{j+1} &= u_i^{j+1}(u_i^{j+1}u_i^{j+1})=u_i^{j+1}\left(2u_i^ju_i^{j+1}-u_i^ju_i^j\right)\\ &=2u_i^j(u_i^{j+1}u_i^{j+1})-(u_i^j)^2u_i^{j+1}\\ &=3(u_i^j)^2u_i^{j+1}-2(u_i^j)^3.\end{aligned} \tag{3.2}$$

Taking $\theta=\frac{1}{2}$ and using it in the above Eqs (3.1) and (3.2), we get

$$u_i^{j+1}-u_i^j+\frac{\gamma\Delta t}{2}(u_{xxxx})_i^{j+1}+\frac{\gamma\Delta t}{2}(u_{xxxx})_i^j-\frac{\Delta t}{2}(u_{xx})_i^{j+1}-\frac{\Delta t}{2}(u_{xx})_i^j+$$
$$\frac{3\Delta t}{2}(u_i^j)^2u_i^{j+1}-\Delta t(u_i^j)^3+\frac{1}{2}-\Delta t(u_i^j)^3-\frac{\Delta t}{2}u_i^{j+1}-\frac{\Delta t}{2}u_i^j=\Delta t f_i^j. \tag{3.3}$$

Simplifying the above equation and manipulating terms, we have

$$(1+\frac{3\Delta t}{2}(u_i^j)^2-\frac{\Delta t}{2})u_i^{j+1}-\frac{\Delta t}{2}(u_{xx})_i^{j+1}+\frac{\gamma\Delta t}{2}(u_{xxxx})_i^{j+1}$$
$$=(1+\frac{1}{2}\Delta t(u_i^j)^2+\frac{\Delta t}{2})u_i^j+\frac{\Delta t}{2}(u_{xx})_i^j-\frac{\gamma\Delta t}{2}(u_{xxxx})_i^j+\hat{f}_i^j. \tag{3.4}$$

Let

$$1+\frac{3\Delta t}{2}(u_i^j)^2-\frac{\Delta t}{2}=A_i^j,\ \text{ and }\ 1+\frac{1}{2}\Delta t(u_i^j)^2+\frac{\Delta t}{2}=B_i^j.$$

Then, the above equation becomes

$$A_i^ju_i^{j+1}-\frac{\Delta t}{2}(u_{xx})_i^{j+1}+\frac{\gamma\Delta t}{2}(u_{xxxx})_i^{j+1}=B_i^ju_i^j+\frac{\Delta t}{2}(u_{xx})_i^j$$
$$-\frac{\gamma\Delta t}{2}(u_{xxxx})_i^j+\hat{f}_i^j. \tag{3.5}$$

Now, using approximated u, u_{xx}, and u_{xxxx} via the QTB-spline collocation technique, we get

$$\left(\tau_1A_i^j-\frac{\Delta t}{2}\tau_6+\frac{\gamma}{2}\Delta t\tau_{11}\right)C_{i-2}^{j+1}+\left(\tau_2A_i^j-\frac{\Delta t}{2}\tau_7+\tau_{12}\frac{\Delta t}{2}\gamma\right)C_{i-1}^{j+1}$$
$$+\left(\tau_3A_i^j-\frac{\Delta t}{2}\tau_8+\tau_{13}\frac{\gamma}{2}\Delta t\right)C_i^{j+1}+\left(\tau_2A_i^j-\frac{\Delta t}{2}\tau_7+\tau_{12}\frac{\Delta t}{2}\gamma\right)C_{i+1}^{j+1}$$
$$+\left(\tau_1A_i^j-\frac{\Delta t}{2}\tau_6+\tau_{11}\frac{\gamma}{2}\Delta t\right)C_{i+2}^{j+1}=\left(\tau_1B_i^j+\frac{\Delta t}{2}\tau_6-\tau_{11}\frac{\Delta t}{2}\gamma\right)C_{i-2}^j$$

$$+\left(\tau_2 B_i^j + \frac{\Delta t}{2}\tau_7 - \tau_{12}\frac{\Delta t}{2}\gamma\right)C_{i-1}^{j+1} + \left(\tau_3 B_i^j + \frac{\Delta t}{2}\tau_8 - \tau_{13}\frac{\Delta t}{2}\gamma\right)C_i^{j+1}$$
$$+\left(\tau_2 B_i^j + \frac{\Delta t}{2}\tau_7 - \tau_{12}\frac{\Delta t}{2}\gamma\right)C_{i+1}^{j+1} + \left(\tau_1 B_i^j + \frac{\Delta t}{2}\tau_6 - \tau_{11}\frac{\Delta t}{2}\gamma\right)C_{i+2}^{j+1} + \hat{f}_i^j. \tag{3.6}$$

We suppose that $\hat{A}_i^j = \tau_1 A_i^j - \frac{\Delta t}{2}\tau_6 + \frac{\gamma}{2}\Delta t\tau_{11}$, $\hat{B}_i^j = \tau_2 A_i^j - \frac{\Delta t}{2}\tau_7 + \frac{\gamma}{2}\Delta t\tau_{12}$,
$\hat{D}_i^j = \tau_3 A_i^j - \frac{\Delta t}{2}\tau_8 + \frac{\gamma}{2}\Delta t\tau_{13}$, $\hat{E}_i^j = \tau_1 B_i^j + \frac{\Delta t}{2}\tau_6 - \frac{\gamma}{2}\Delta t\tau_{11}$,
$\hat{F}_i^j = \tau_2 B_i^j + \frac{\Delta t}{2}\tau_7 - \frac{\gamma}{2}\Delta t\tau_{12}$, and $\hat{G}_i^j = \tau_3 B_i^j + \frac{\Delta t}{2}\tau_8 - \frac{\gamma}{2}\Delta t\tau_{13}$.
Then, the above equation becomes

$$\hat{A}_i^j c_{i-2}^{j+1} + \hat{B}_i^j c_{i-1}^{j+1} + \hat{D}_i^j c_i^{j+1} + \hat{B}_i^j c_{i+1}^{j+1} + \hat{A}_i^j c_{i+2}^{j+1} = \hat{E}_i^j c_{i-2}^j + \hat{F}_i^j c_{i-1}^j +$$
$$\hat{G}_i^j c_i^j + \hat{F}_i^j c_{i+1}^j + \hat{E}_i^j c_{i+2}^j + \hat{f}_i^j, \quad i = 2, 3, ..., M-2, \quad j = 0, 1, ..., N. \tag{3.7}$$

The discretization of the BCs is as follows:

$$u(a,t) = \psi_1(t) \Rightarrow \tau_1 C_{-2}^j + \tau_2 C_{-1}^j + \tau_3 C_0^j + \tau_2 C_1^j + \tau_1 C_2^j = \psi_1^j, \tag{3.8}$$

$$u(b,t) = \psi_2(t) \Rightarrow \tau_1 C_{M-2}^j + \tau_2 C_{M-1}^j + \tau_3 C_M^j + \tau_2 C_{M+1}^j + \tau_1 C_{M+2}^j = \psi_2^j, \tag{3.9}$$

$$u_{xx}(a,t) = 0 \Rightarrow \tau_6 C_{-2}^j + \tau_7 C_{-1}^j + \tau_8 C_0^j + \tau_7 C_1^j + \tau_6 C_2^j = 0, \tag{3.10}$$

and

$$u_{xx}(b,t) = 0 \Rightarrow \tau_6 C_{M-2}^j + \tau_7 C_{M-1}^j + \tau_8 C_M^j + \tau_7 C_{M+1}^j + \tau_6 C_{M+2}^j = 0. \tag{3.11}$$

Solving Eqs (3.8)–(3.11), we have

$$C_{-1}^j = \frac{\hat{\tau_P}}{\hat{\tau_m}} C_0^j - C_1^j + \frac{\hat{\tau_6}}{\hat{\tau_m}}\psi_1^j, \tag{3.12}$$

$$C_{-2}^j = \frac{\hat{\tau_q}}{\hat{\tau_m}} C_0^j - C_2^j - \frac{\tau_7}{\hat{\tau_m}}\psi_1^j, \tag{3.13}$$

$$C_{M+1}^j = -c_{M-1}^j - \frac{\hat{\tau_p}}{\hat{\tau_m}} C_M^j + \frac{\tau_6}{\hat{\tau_m}}\psi_2^j, \tag{3.14}$$

$$C_{M+2}^j = -C_{M-2}^j + \frac{\hat{\tau_q}}{\hat{\tau_m}} C_M^j - \frac{\tau_7}{\hat{\tau_m}}\psi_2^j, \tag{3.15}$$

where $\hat{\tau_m} = \tau_2\tau_6 - \tau_1\tau_7$, $\hat{\tau_p} = \tau_3\tau_6 - \tau_1\tau_8$, and $\hat{\tau_q} = \tau_3\tau_7 - \tau_2\tau_8$.
For $i = 0$, using Eqs (3.12) and (3.13) in (3.7) and manipulating terms, we get

$$\left(\frac{\hat{\tau_q}}{\hat{\tau_m}}\hat{A}_0^j - \frac{\hat{\tau_p}}{\hat{\tau_m}}\hat{B}_0^j + \hat{D}_0^j\right)C_0^{j+1} = \left(\frac{\hat{\tau_q}}{\hat{\tau_m}}\hat{E}_0^j - \frac{\hat{\tau_p}}{\hat{\tau_m}}\hat{F}_0^j + \hat{G}_0^j\right)C_0^j + \frac{\tau_7}{\hat{\tau_m}}\hat{A}_0^j\psi_1^{j+1} -$$

$$\frac{\tau_6}{\hat{\tau_m}}\hat{B}_0^j\psi_1^{j+1} - \frac{\tau_7}{\hat{\tau_m}}\hat{E}_0^j\psi_1^j + \frac{\tau_6}{\hat{\tau_m}}\hat{F}_0^j\psi_1^j + \hat{f}_0^j, \quad j = 0, 1, 2, ..., N. \tag{3.16}$$

For $i = 1$, using Eq (3.12) in (3.7), we get

$$\begin{aligned}\left(-\frac{\hat{\tau_p}}{\hat{\tau_m}}\hat{A}_1^j + \hat{B}_1^j\right)C_0^{j+1} + \left(-\hat{A}_1^j + \hat{D}_1^j\right)C_1^{j+1} + B_1^j C_2^{j+1} + A_1^j C_3^{j+1}\\ = \left(-\frac{\hat{\tau_p}}{\hat{\tau_m}}\hat{E}_1^j + \hat{F}_1^j\right)C_0^j + \left(-\hat{E}_1^j + \hat{G}_1^j\right)C_1^j + \hat{F}_1^j C_2^j + \hat{E}_1^j C_3^j - \frac{\tau_6}{\hat{\tau_m}}\hat{A}_1^j\psi_1^{j+1}\\ + \frac{\tau_6}{\hat{\tau_m}}\hat{E}_1^j\psi_1^j + \hat{f}_1^j, \quad j = 0, 1, 2, ..., N.\end{aligned} \tag{3.17}$$

For $i = M - 1$, using Eq (3.13) in (3.7), we get

$$\begin{aligned}\hat{A}_{M-1}^j C_{M-3}^{j+1} + \hat{B}_{M-1}^j C_{M-2}^{j+1} + \left(-\hat{A}_{M-1}^j + \hat{D}_{M-1}^j\right)C_{M-1}^{j+1} + \left(-\frac{\hat{\tau_p}}{\hat{\tau_m}}\hat{A}_{M-1}^j + \hat{B}_{M-1}^j\right)C_M^{j+1}\\ = \hat{E}_{M-1}^j C_{M-3}^j + \hat{F}_{M-1}^j C_{M-2}^j + \left(-\hat{E}_{M-1}^j\hat{G}_{M-1}^j\right)C_{M-1}^j + \left(-\frac{\hat{\tau_p}}{\hat{\tau_m}}\hat{E}_{M-1}^j + \hat{F}_{M-1}^j\right)C_M^j\\ - \frac{\tau_6}{\hat{\tau_m}}\hat{A}_{M-1}^j\psi_2^{j+1} - \frac{\tau_6}{\hat{\tau_m}}\hat{E}_{M-1}^j\psi_2^j + \hat{f}_i^j, \quad j = 1, 2, ..., N.\end{aligned} \tag{3.18}$$

For $i = M$, using Eq (3.13) and (3.14) in (3.7), we get

$$\begin{aligned}\left(\frac{\hat{\tau_q}}{\hat{\tau_m}}\hat{A}_M^j - \frac{\hat{\tau_p}}{\hat{\tau_m}}\hat{B}_M^j + \hat{D}_M^j\right)C_M^{j+1}\\ \left(\frac{\hat{\tau_q}}{\hat{\tau_m}}\hat{E}_M^j - \frac{\hat{\tau_p}}{\hat{\tau_m}}\hat{F}_M^j + \hat{G}_M^j\right)C_M^j - \frac{\tau_6}{\hat{\tau_m}}B_M^j\psi_2^{j+1} + \frac{\tau_7}{\hat{\tau_m}}A_M^j\psi_2^{j+1}\\ + \frac{\tau_6}{\hat{\tau_m}}F_M^j\psi_2^j - \frac{\tau_7}{\hat{\tau_m}}E_M^j\psi_2^j + \hat{f}_M^j, \quad j = 0, 1, ..., N.\end{aligned} \tag{3.19}$$

At the time t^j, $j = 0, 1, ..., N$, and Eqs (3.16), (3.17), (3.7), (3.18), and (3.19) form a linear system of $(M + 1) \times (M + 1)$ order. We must establish the initial vectors $\left(C_0^0, C_1^0, ..., C_{M-1}^0, C_M^0\right)$ from the IC to solve the system with the $M + 1$ equation and $M + 3$ unknowns. To remove the C_{-1}^0 and C_{M+1}^0, we use the IC $u(x, 0) = \phi(x)$ and its first and second derivatives at boundaries as follows:

$$u(x, 0) = \phi(x) \Rightarrow \tau_1 C_{i-2}^0 + \tau_2 C_{i-1}^0 + \tau_3 C_i^0 + \tau_2 C_{i+1}^0 + \tau_1 C_{i+2}^0 = \phi(x_i), \tag{3.20}$$

$$u_x(a, 0) = \phi_x(a) \Rightarrow -\tau_4 C_2^0 - \tau_5 C_{-1}^0 + \tau_5 C_1^0 + \tau_4 C_2^0 = \phi_x(a), \tag{3.21}$$

$$u_x(b, 0) = \phi_x(b) \Rightarrow -\tau_4 C_{M-2}^0 - \tau_5 C_{M-1}^0 + \tau_5 C_{M+1}^0 + \tau_4 C_{M+2}^0 = \phi_x(b), \tag{3.22}$$

$$u_{xx}(a, 0) = \phi_{xx}(a) \Rightarrow \tau_6 C_{-2}^0 + \tau_7 C_{-1}^0 + \tau_8 C_0^0 + \tau_7 C_1^0 + \tau_6 C_2^0 = \phi_{xx}(a), \tag{3.23}$$

$$u_{xx}(b, 0) = \phi_{xx}(b) \Rightarrow \tau_6 C_{M-2}^0 + \tau_7 C_{M-1}^0 + \tau_8 C_M^0 + \tau_7 C_{M+1}^0 + \tau_6 C_{M+2}^0 = \phi_{xx}(b). \tag{3.24}$$

Solving Eqs (3.20)–(3.24), we get

$$C_{-1}^0 = \frac{\tau_4\tau_8}{\eta_4}C_0^0 + \frac{\eta_3}{\eta_4}C_1^0 + \frac{2\tau_4\tau_6}{\eta_4}C_2^0 - \frac{1}{\eta_4}\left(\tau_6\phi_x(a) + \tau_4\phi_{xx}(a)\right), \tag{3.25}$$

$$C_{-2}^0 = \frac{\tau_5\tau_8}{\eta_4}C_0^0 + \frac{2\tau_5\tau_7}{\eta_4}C_1^0 + \frac{\eta_3}{\eta_4}C_2^0 - \frac{1}{\eta_4}\left(\tau_7\phi_x(a) + \tau_5\phi_{xx}(a)\right), \tag{3.26}$$

$$C_{M+1}^0 = \frac{2\tau_4\tau_6}{\eta_4}C_{M-2}^0 + \frac{\eta_3}{\eta_4}C_{M-1}^0 + \frac{\tau_4\tau_8}{\eta_4}C_M^0 + \frac{1}{\eta_4}\left(\tau_6\phi_x(b) + \tau_4\phi_{xx}(b)\right), \tag{3.27}$$

$$C_{M+2}^0 = \frac{\eta_3}{\eta_4}C_{M-2}^0 + \frac{2\tau_5\tau_7}{\eta_4}C_{M-1}^0 + \frac{\tau_5\tau_8}{\eta_4}C_M^0 + \frac{1}{\eta_4}\left(\tau_7\phi_x(b) - \tau_5\phi_{xx}(b)\right), \tag{3.28}$$

where $\tau_5\tau_6 + \tau_4\tau_7 = \eta_3$ and $\tau_5\tau_6 - \tau_4\tau_7 = \eta_4$.
For $i = 0$, using (3.25) and (3.26) in (3.20), we get

$$\left(\tau_1\frac{\tau_5\tau_8}{\eta_4} + \tau_2\frac{\tau_4\tau_8}{\eta_4} + \tau_3\right)C_0^0 + \left(2\tau_1\frac{\tau_5\tau_7}{\eta_4} + \tau_2\frac{\eta_3}{\eta_4} + \tau_2\right)C_1^0 + \left(2\tau_2\frac{\tau_4\tau_6}{\eta_4} + \tau_1\frac{\eta_3}{\eta_4} + \tau_1\right)C_2^0 = u_0(x_0) + \frac{\tau_1}{\eta_4}\left(\tau_7\psi_x(a) + \tau_5\psi_{xx}(a)\right) + \frac{\tau_2}{\eta_4}\left(\tau_6\phi_x(a) + \tau_4\phi_{xx}(a)\right). \tag{3.29}$$

For $i = 1$, using (3.25) in (3.20), we get

$$\left(\tau_1\frac{\tau_4\tau_8}{\eta_4} + \tau_2\right)C_0^0 + \left(\tau_1\frac{\eta_3}{\eta_4} + \tau_3\right)C_1^0 + \left(2\tau_1\frac{\tau_4\tau_6}{\eta_4} + \tau_2\right)C_2^0 + \tau_1C_3^0 = u_0(x_1) + \frac{\tau_1}{\eta_4}\left(\tau_6\phi_x(a) + \tau_4\phi_{xx}(a)\right). \tag{3.30}$$

For $i = M - 1$, using (3.27) in (3.20), we get

$$\tau_1C_{M-3}^0 + \left(2\tau_1\frac{\tau_4\tau_6}{\eta_4} + \tau_2\right)C_{M-2}^0 + \left(\tau_1\frac{\eta_3}{\eta_4} + \tau_3\right)C_{M-1}^0 + \left(\tau_1\frac{\tau_4\tau_8}{\eta_4} + \tau_2\right)C_M^0 = u_0(x_{M-1}) - \frac{\tau_1}{\eta_4}\left(\tau_6\phi_x(b) - \tau_4\phi_{xx}(b)\right). \tag{3.31}$$

For $i = M$, using (3.27) and (3.29) in (3.20), we get

$$\left(\tau_1\frac{\eta_3}{\eta_4} + 2\tau_2\frac{\tau_4\tau_6}{\eta_4} + \tau_1\right)C_{M-2}^0 + \left(2\tau_1\frac{\tau_5\tau_7}{\eta_4} + \tau_2\frac{\eta_3}{\eta_4} + \tau_2\right)C_{M-1}^0 + \left(\tau_1\frac{\tau_5\tau_8}{\eta_4} + \tau_2\frac{\tau_4\tau_8}{\eta_4} + \tau_3\right)C_M^0 = u_0(x_M) - \frac{\tau_1}{\eta_4}\left(\tau_7\psi_x(b) - \tau_5\psi_{xx}(b)\right) - \frac{\tau_1}{\eta_4}\left(\tau_6\phi_x(b) - \tau_4\phi_{xx}(b)\right). \tag{3.32}$$

Equations (3.25), (3.26), (3.20), (3.27), and (3.29) form a system $(M+1)\times(M+1)$ order at the time t^0.

4. Analysis of stability

This section goes into stability analysis for the discretized system of the extended F-K equation via the von Neumann method [35]. According to the Duhamels' principle [36], the stability analysis of an inhomogeneous problem follows promptly from the homogeneous one. Thus, it seems necessary to examine the stability of the discretized system for the extended F-K equation with the force function $f = 0$. Taking $\theta = \frac{1}{2}$ and linearizing the nonlinear term u^3 by taking $u^2 = \hat{k}_1^2$ as a locally constant, the Eq (3.1) can be written as

$$u_i^{j+1} - u_i^j + \gamma\frac{\Delta t}{2}(u_{xxxx})_i^j + \frac{\gamma}{2}\Delta t(u_{xxxx})_i^j - \frac{\Delta t}{2}(u_{xx})_i^{j+1} - \frac{\Delta t}{2}(u_{xx})_i^j\hat{k}_{i-1}^2\left(\frac{u_i^{j+1}+u_i^j}{2}\right)\Delta t = 0. \tag{4.1}$$

The above equation can be written as

$$\bar{A}u_i^{j+1} = \frac{\Delta t}{2}(u_{xx})_i^{j+1} + \gamma\frac{\Delta t}{2}(u_{xxxx})_i^{j+1} = \bar{B}u_i^j = \frac{\Delta t}{2}(u_{xx})_i^j + \gamma\frac{\Delta t}{2}(u_{xxxx})_i^j, \tag{4.2}$$

where

$$\left(1 + \frac{\hat{k}_1^2 - 1}{2}\right) = \bar{A}, \text{ and } \left(1 - \frac{\hat{k}_1^2 - 1}{2}\right) = \bar{B}.$$

Now, using approximated values of u, u_{xx}, and u_{xxxx} by the QTB-spline collocation technique in Eq (4.2), we get

$$A^*C_{i-2}^{j+1} + B^*C_{i-1}^{j+1} + D^*C_i^{j+1} + B^*C_{i+1}^{j+1} + A^*C_{i+1}^{j+1} = E^*C_{i-2}^j + F^*C_{i-1}^j + G^*C_i^j + F^*C_{i+1}^j + E^*C_{i+1}^j, \tag{4.3}$$

where

$$A^* = \tau_1\bar{A} - \frac{\Delta t}{2}\tau_6 + \frac{\gamma}{2}\Delta t\tau_{11},\ B^* = \tau_2\bar{A} - \frac{\Delta t}{2}\tau_7 + \frac{\gamma}{2}\Delta t\tau_{12},$$
$$D^* = \tau_3\bar{A} - \frac{\Delta t}{2}\tau_7 + \frac{\gamma}{2}\Delta t\tau_{13},\ E^* = \tau_1\bar{B} - \frac{\Delta t}{2}\tau_6 + \frac{\gamma}{2}\Delta t\tau_{11},$$
$$F^* = \tau_2\bar{B} - \frac{\Delta t}{2}\tau_7 + \frac{\gamma}{2}\Delta t\tau_{12}, \text{ and, } G^* = \tau_3\bar{B} - \frac{\Delta t}{2}\tau_8 + \frac{y}{2}\Delta t\tau_{13}.$$

We suppose one Fourier mode from the full solution $C_i^j = \delta^j e^{\kappa i\vartheta}$ is used as trial solutions at x_i, where $\vartheta = \varepsilon h$. The h is the element size, ε is the mode number, and $\kappa = \sqrt{-1}$. Inverting this solution in Eq (4.3), we have

$$(2A^*cos(2\epsilon h) + 2B^*cos(\epsilon h) + D^*)\,\delta^{j+1} = (2E^*cos(2\epsilon h) + 2F^*cos(\epsilon h) + G^*)\,\delta^j. \tag{4.4}$$

Simplifying and manipulating some terms, we have

$$\delta = \frac{4E^*cos^2(\epsilon h) + 2F^*cos^2(\frac{\epsilon h}{2}) - (2E^* + 2F^* - G^*)}{4A^*cos^2(\epsilon h) + 2B^*cos^2(\frac{\epsilon h}{2}) - (2A^* + 2B^* - D^*)}, \tag{4.5}$$

where,

$$A^* = \left(\frac{1+\hat{k}^2}{2}\right)\tau_1 + \frac{\Delta t}{2}(\gamma\tau_{11} - \tau_6),\ B^* = \left(\frac{1+\hat{k}^2}{2}\right)\tau_2 + \frac{\Delta t}{2}(\gamma\tau_{12} - \tau_7),$$
$$D^* = \left(\frac{1+\hat{k}^2}{2}\right)\tau_3 + \frac{\Delta t}{2}(\gamma\tau_{13} - \tau_8),\ E^* = \left(\frac{3-\hat{k}^2}{2}\right)\tau_1 - \frac{\Delta t}{2}(\gamma\tau_{11} - \tau_6),$$
$$F^* = \left(\frac{3-\hat{k}^2}{2}\right)\tau_2 - \frac{\Delta t}{2}(\gamma\tau_{12} - \tau_7),\ G^* = \left(\frac{3-\hat{k}^2}{2}\right)\tau_3 - \frac{\Delta t}{2}(\gamma\tau_{13} - \tau_8).$$

Inverting values of coefficients, we observe that $E^* \leq A^*$, $F^* \leq B^*$, $G^* \leq D^*$, and, so, $|\delta| \leq 1$. Therefore, the extended F-K equation discretized system is unconditionally stable.

5. Computational results

Example 1. Consider extended F-K Eq (1.1) in $x \in [-4, 4]$ with the IC as

$$u(x, 0) = -\sin \pi x, \quad x \in [-4, 4],$$

and the BCs as

$$u(-4, t) = 0, \quad u_{xx}(-4, t) = 0, \quad u(4, t) = 0, \quad u_{xx}(4, t) = 0.$$

Figures 1(a)–(c) illustrate the computations for $h = 0.1$, $\Delta t = 0.001$ at $t = 0$, 0.05, 0.1, 0.15, and 2.0 for $\gamma = 0.0001$ and $\gamma = 0.001$, respectively. The figures indicate that solutions are identical for $\gamma = 0.0001$ and $\gamma = 0.001$, whereas solutions for $\gamma = 0.1$ rapidly decrease toward 0, confirming the extended F-K equation's stabilizing property. The solutions that are acquired efficiently reproduce the satisfactory qualitative properties of the extended F-K equation. Figures 2(a)–(c) depict the three-dimensional visualization of numerical solutions for different values of γ ($\gamma = 0.0001$, $\gamma = 0.001$, and $\gamma = 0.1$) at $t = 0.2$, with $h = 0.1$ and $\Delta t = 0.001$. It can be noted from these figures that the outcome of solutions is nearly identical for very small values of γ. However, the deterioration of solutions to zero is very immediate in the case of $\gamma = 0.1$, which proves the stabilizing nature of the extended F-K equation. Table 2 presents a comparison between the current approach and existing methods in terms of L_2 and L_∞ error norms. The comparison is made with a value of $\Delta t = 0.001$, $\gamma = 0.1$, and $t = 0.2$. At $M = 20$, our technique surpasses quartic B-spline differential quadrature method (QAB-DQM) [30], QBCM [11], and modified cubic B-spline based differential quadrature method (MCB-DQM) [8] in terms of outcomes. Furthermore, our study shows that our results exhibit greater performance compared to the findings in QBDQM [10] in terms of L_2 error norms. Therefore, we are able to conclude that the approach yields better results compared to certain methods described in the literature for a small grid size.

Table 2. The error norms L_2 and L_∞ for Example 1 with $\gamma = 0.1$ and $\Delta t = 0.001$ at $t = 0.2$.

Methods	Error norms	M =20	M =40	M =80
Projected method	L_2	6.401e-03	1.9524e-02	5.839e-04
	L_∞	2.796e-03	6.449e-03	2.574e-04
QAB-DQM [30]	L_2	1.62e-02	8.91e-03	2.92e-03
	L_∞	1.31e-02	7.94e-03	2.76e-03
QBDQM [10]	L_2	2.135e-02	2.216e-03	3.123e-04
	L_∞	1.155e-03	1.224e-03	1.531e-04
QBCM [11]	L_2	1.116e-02	2.815e-03	5.657e-04
	L_∞	5.510e-03	1.339e-03	2.834e-04
MCB-DQM [8]	L_2	1.888e-02	2.300e-03	2.400e-04
	L_∞	1.184e-02	2.220e-03	2.300e-04

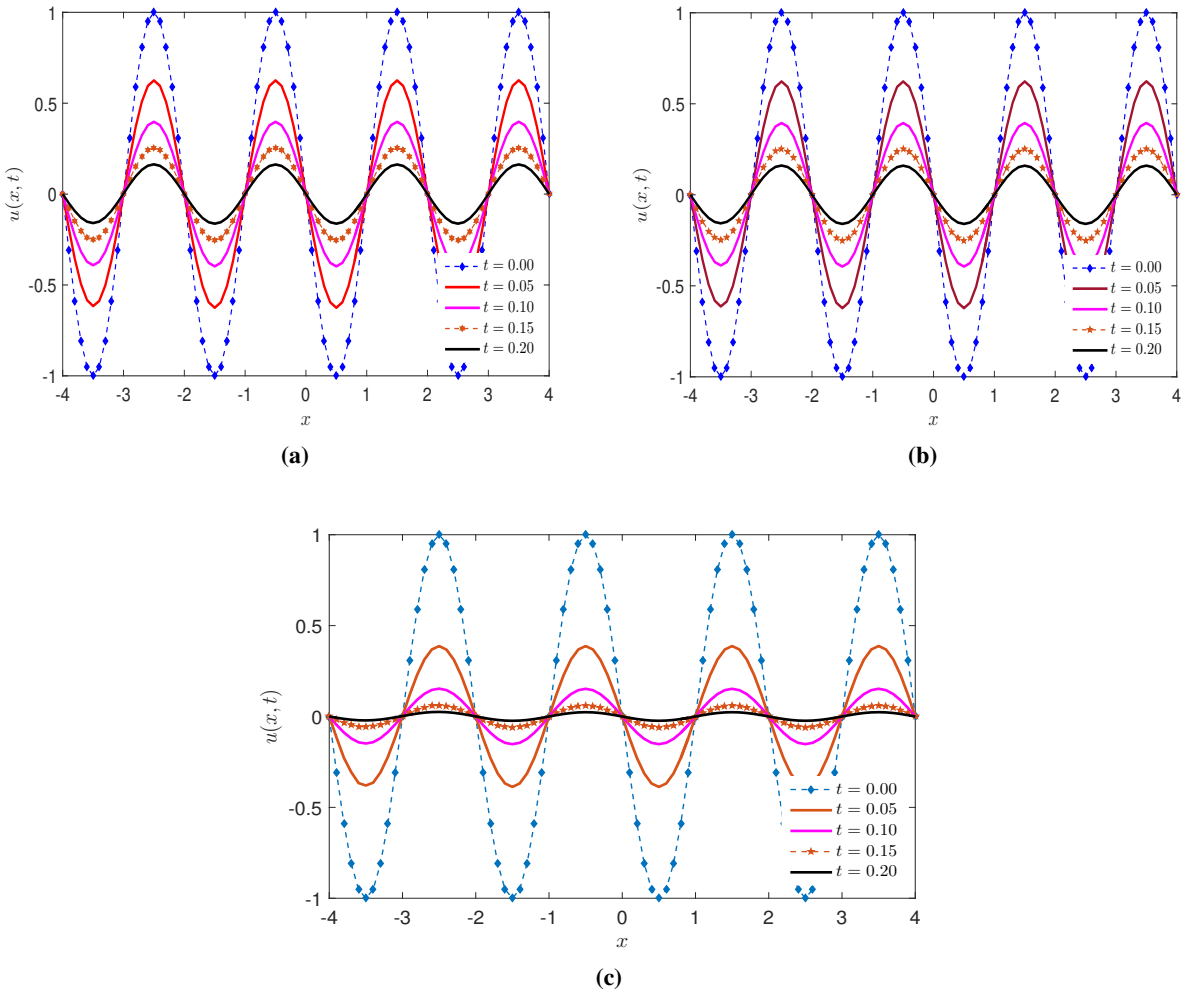

Figure 1. Simulation of Example 1 with (a) $\gamma = 0.0001$, (b) $\gamma = 0.001$, and (c) $\gamma = 0.1$ for $h = 0.1$ and $\Delta t = 0.001$ at various t.

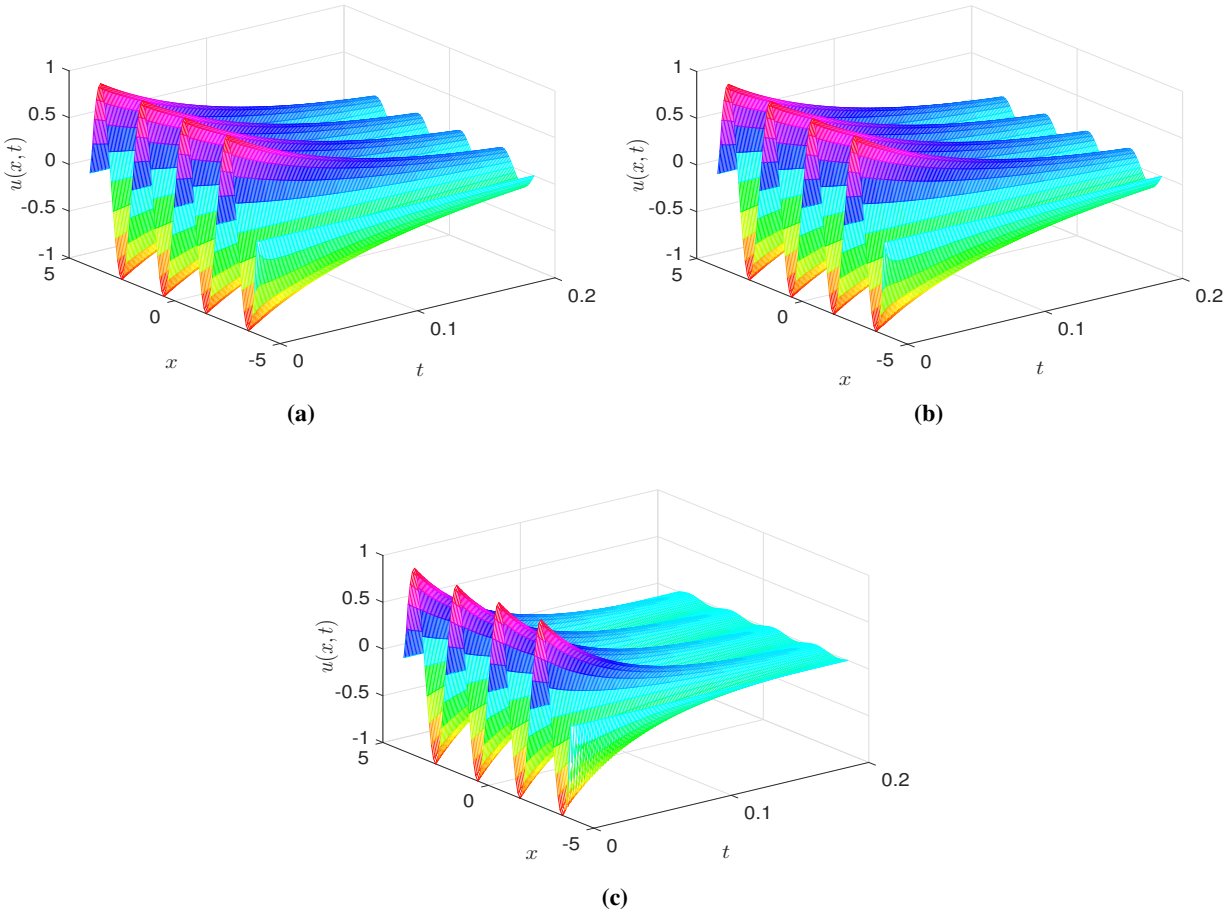

Figure 2. 3D plots of $u(x,t)$ for Example 1 with (a) $\gamma = 0.0001$, (b) $\gamma = 0.001$, and (c) $\gamma = 0.1$ for $h = 0.1$ and $\Delta t = 0.001$ at $t = 0.2$.

Example 2. Consider the extended F-K Eq (1.1) in $x \in [-4, 4]$ with the IC as

$$u(x, 0) = 10^{-3} \exp\left(-x^2\right), \quad x \in [-4, 4],$$

and the BCs as

$$u(-4, t) = 1, \quad u_{xx}(-4, t) = 0, \quad u(4, t) = 1, \quad u_{xx}(4, t) = 0.$$

Figure 3 illustrates the computations for $h = 0.1$, $\Delta t = 0.001$ at $t = 0.25$, 1, 1.75, 2.5, 3.5, and 4.5 for $\gamma = 0.0001$. This figure shows that solutions decay and reach a stable state approaching the value 1 as time increases, which is the instant replicate of the adequate qualitative performance of the extended F-K equation. Figure 4 illustrates the 3D view of the computations with $\gamma = 0.0001$, $h = 0.025$, and $\Delta t = 0.0001$ for $t \in [0.25, 5]$. It is also obvious from this figure that solutions start to decay and reach a stable state, approaching the value 1 as time increases. Table 3 presents the L_2 and L_∞ error norms, in addition to the R_c, for the parameters $\gamma = 0.0001$ and $\Delta t = 0.0001$ at $t = 1$ and $t = 4.5$. The table shows a decrease in error norms as the mesh size increases. Additionally, it is noted that error norms are at their minimum at time t=4.5, indicating that the extended F-K equation is in a stable state. Furthermore, the accuracy of the projected procedure in space variables is second order.

Table 3. The error norms L_2 and L_∞ for Example 2, convergence rate with $\gamma = 0.0001$, $\Delta t = 0.0001$ at $t = 1$ and $t = 4.5$.

M	$t = 1$				$t = 4.5$			
	L_2	R_c	L_∞	R_c	L_2	R_c	L_∞	R_c
20	2.909e-02	–	9.708e-03	–	1.265e-03	–	4.039e-04	–
40	9.250e-03	1.65	2.192e-03	2.15	3.437e-04	1.88	7.981e-05	2.34
80	2.587e-03	1.84	4.354e-04	2.33	9.182e-05	1.90	1.520e-05	2.39

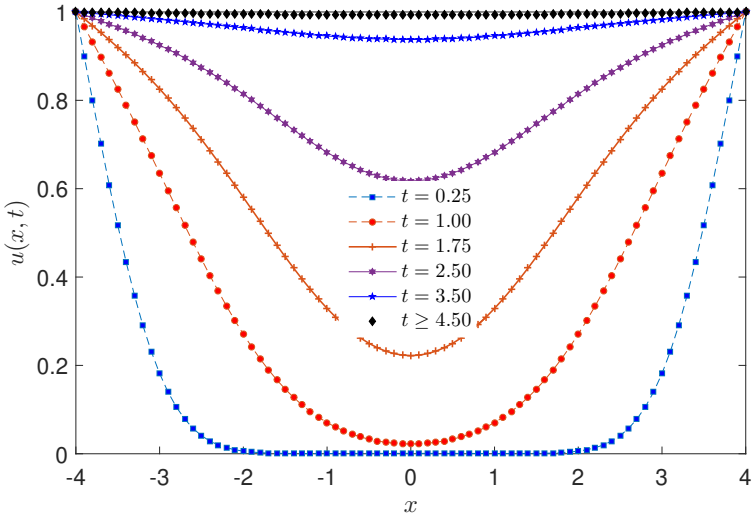

Figure 3. Plots for Example 2 with $\gamma = 0.0001$, $h = 0.1$, and $\Delta t = 0.001$ at different t.

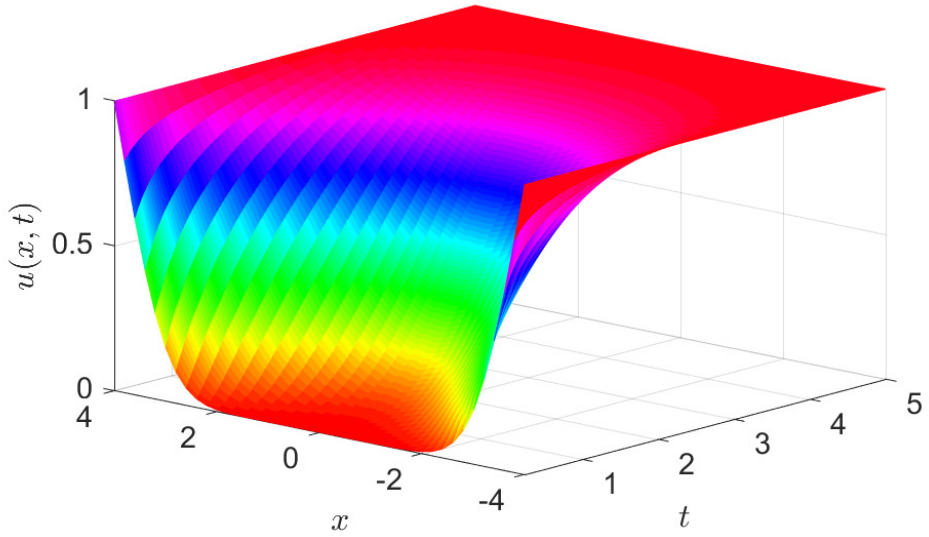

Figure 4. 3D plots of $u(x,t)$ for Example 2 with $\gamma = 0.0001$ for $h = 0.025$, and $\Delta t = 0.0001$, where $t \in [0.25, 5]$.

Example 3. Consider the extended F-K Eq (1.1) in $x \in [-4, 4]$ with the IC as

$$u(x, 0) = -10^{-3} \exp\left(-x^2\right), \quad x \in [-4, 4],$$

and the BCs

$$u(-4, t) = -1, \quad u_{xx}(-4, t) = 0, \quad u(4, t) = -1, \quad u_{xx}(4, t) = 0.$$

Figure 5 illustrates the computations for $h = 0.1$, $\Delta t = 0.001$ at $t = 0.25$, 1, 1.75, 2.5, 3.5, and 4.5 for $\gamma = 0.0001$. Figure 6 depicts the 3D view of the numerical solutions with $\gamma = 0.0001$, $\Delta t = 0.0001$, and $h = 0.025$ for $t \in [0.25, 5]$. It is obvious from these figures that solutions start decaying and reach a stable state approaching the value -1 as time increases, which is the instant replication of the adequate qualitative performance of the extended F-K equation.

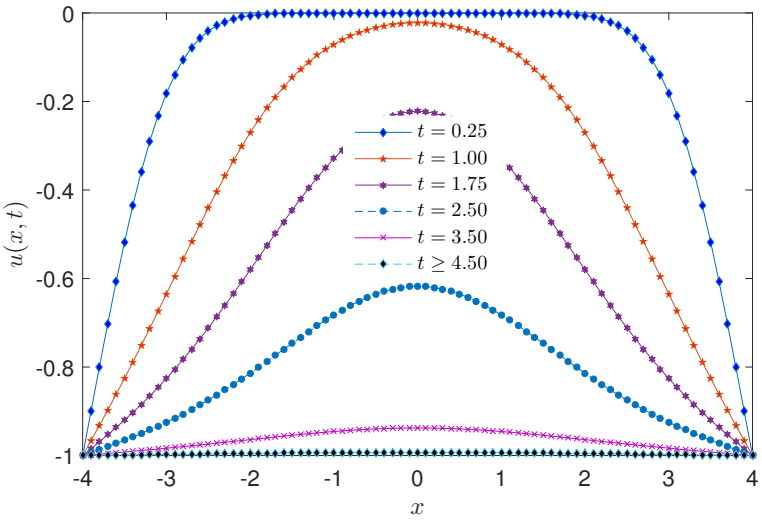

Figure 5. Plots for Example 3 with $\gamma = 0.0001$, $h = 0.1$, and $\Delta t = 0.001$ at different t.

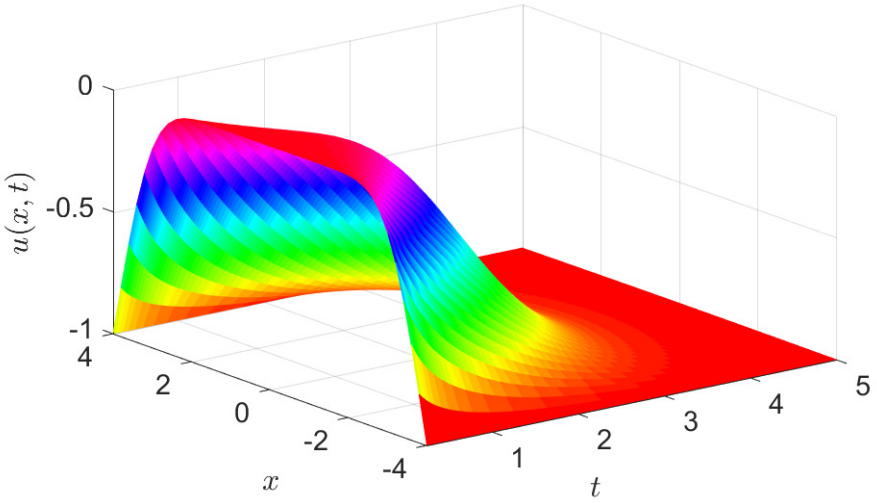

Figure 6. 3D plots of $u(x, t)$ for Example 3 with $\gamma = 0.0001$ for $h = 0.025$, and $\Delta t = 0.0001$, where $t \in [0.25, 5]$.

Example 4. Lastly, we look at the nonhomogenous extended F-K equation

$$u_t + \gamma u_{xxxx} - u_{xx} + f(u) = g(x,t), \quad x \in [0,1], \quad t \in [0,1],$$

with

$$u(x,t) = e^{-t} sin(2\pi x),$$

and BCs

$$u(0,t) = 0, \quad u_{xx}(0,t) = 0, \quad u(1,t) = 0, \quad u_{xx}(1,t) = 0,$$

where $f(u) = u^3 - u$ and $g(x,t) = e^{-t} sin(2\pi x)(e^{-2t} sin^2(2\pi x) + 4\pi^2 + 16\pi^4 - 2)$.

Table 4 shows L_2 and L_∞ error norms as well as numerical convergence R_c for $\gamma = 1$, $\Delta t = 0.01$ at $t = 0.5$ and $t = 1$. The table clearly indicates that error norms are negligible and decrease as mesh sizes expand. Additionally, the proposed method converges to a space variable of the second order. Figure 7 depicts exact and computation $u(x,t)$ for $\gamma = 1$, and $\Delta t = 0.001$ for $h = 0.025$ with $t = 0.1$, 0.3, 0.5, and 0.7, while Figure 8 depicts 3D plots of exact and computation $u(x,t)$ with $\gamma = 1$, $\Delta t = 0.0005$ for $h = 0.05$ and $t \in [0.02]$, and $h = 0.025$ and $t \in [0,1]$, respectively. These figures show excellent agreement between extact and computation solutions. The absolute error norms are also publicized in Figure 8, which are approximately in 10^{-3}.

Table 4. The error norms L_2 and L_∞ for Example 4, convergence rate with $\gamma = 1$, $\Delta t = 0.01$ at $t = 0.5$ and $t = 1$.

M	$t = 0.5$				$t = 1$			
	L_2	R_c	L_∞	R_c	L_2	R_c	L_∞	R_c
20	8.675e-02	–	2.664e-02	–	1.428e-01	–	4.414e-02	–
25	5.057e-02	2.42	1.425e-02	2.80	8.270e-02	2.45	2.312e-02	2.90
40	1.930e-02	2.01	5.192e-03	2.15	2.708e-02	2.37	6.551e-03	2.68

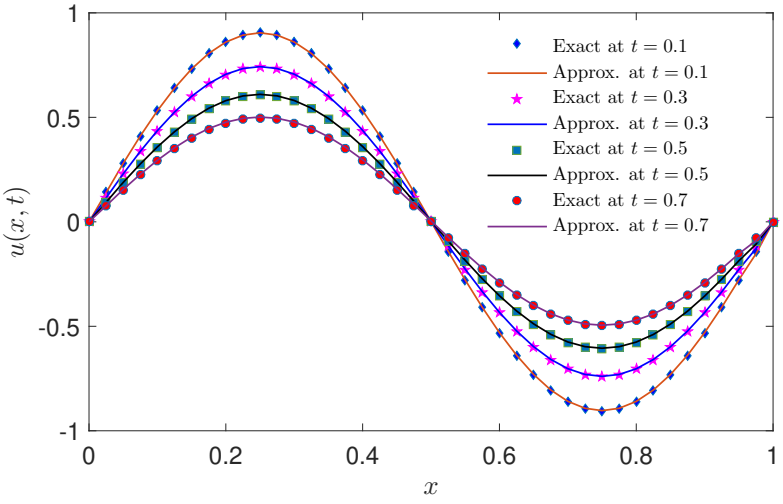

Figure 7. A comparison of the exact and numerical values of $u(x,t)$ for Example 4 with $\gamma = 1$, $h = 0.025$, and $\Delta t = 0.001$ for t=0.1, 0.3, 0.5, 0.7.

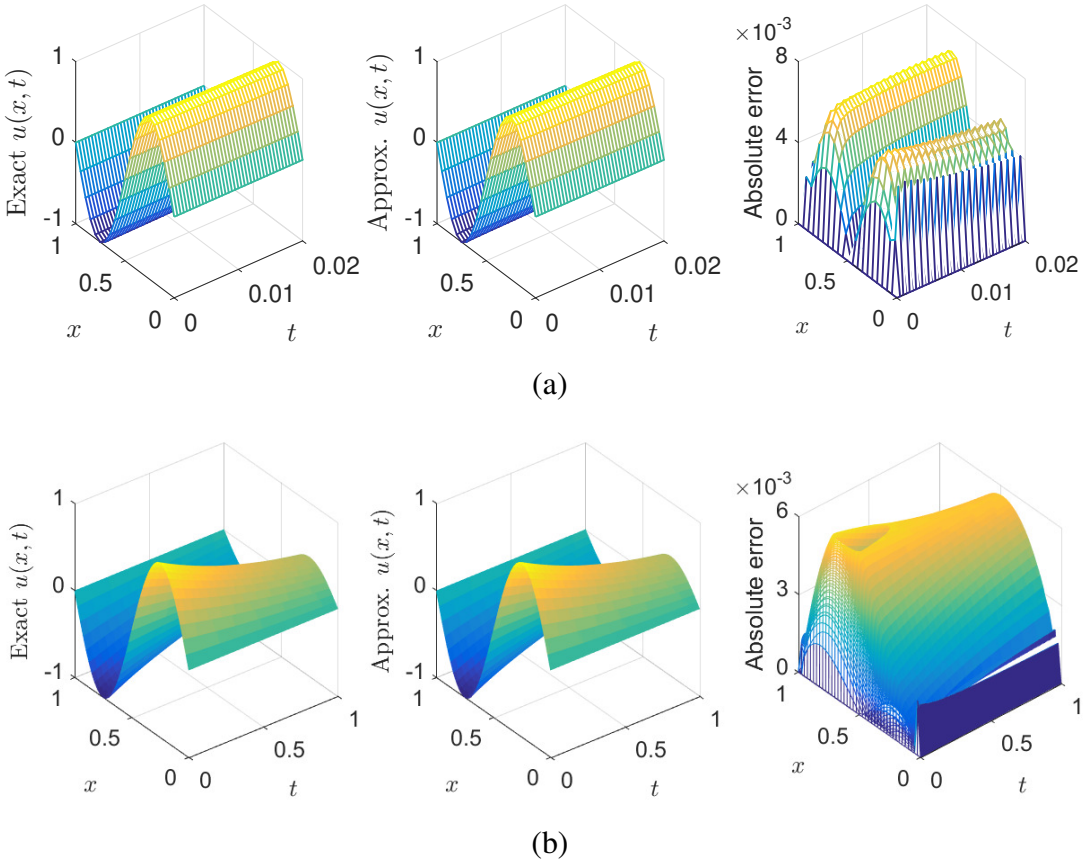

Figure 8. 3D plots of exact and numerical $u(x,t)$ together with abs. norms for $\gamma = 1$ and $\Delta t = 0.0005$ with (a) $h = 0.05$ and $t \in [0, 0.02]$, (b) $h = 0.025$ and $t \in [0, 1]$ for Example 4.

6. Conclusions

A collocation technique based on QTB-spline functions is reported for homogeneous as well as nonhomogeneous extended F-K equations. The nonlinear term is handled by the Rubin-Graves (R-G) type linearization process. To validate results and check efficiency, three examples of homogeneous and one example of nonhomogeneous extended F-K equations are considered. The projected method has been found to yield improved results in comparison to the methods described in [8, 10, 11, 30]. The performance of the projected technique and a relative investigation are accomplished graphically. Figures 1 and 2 portray that the nature of solutions is nearly similar for $\gamma = 0.0001$ and $\gamma = 0.001$ while, for $\gamma = 0.1$, solutions decompose rapidly to 0, ensuring the stability of the extended F-K equation. Figures 3 and 5 portray that solutions decay and attain a stable state approaching the values 1 and -1, respectively, as time increases, which is the instant replicate of the adequate qualitative performance of the extended F-K equation. Figure 8 shows excellent agreement between exact and numerical solutions, with absolute error norms of approximately 10^{-3}. We show that the projected technique is unconditionally stable for the discretized extended F-K equations. Additionally, the technique is determined to be accurate to a second order in space. The numerical analysis proves the projected technique is straightforward and yields very accurate results.

Author contributions

All authors of this article have been contributed equally. All authors have read and approved the final version of the manuscript for publication.

Use of AI tools declaration

The authors declare they have not used Artificial Intelligence (AI) tools in the creation of this article.

Acknowledgements

The authors extend their appreciation to the Deputyship for Research and Innovation, Ministry of Education in Saudi Arabia, for funding this research work through the project number ISP-2024.

Conflict of interest

The authors declare no conflict of interest.

References

1. J. Belmonte-Beitia, G. F. Calvo, V. M. Pérez-García, Effective particle methods for Fisher-Kolmogorov equations: Theory and applications to brain tumor dynamics, *Commun. Nonlinear Sci. Numer. Simul.*, **19** (2014), 3267–3283. https://doi.org/10.1016/j.cnsns.2014.02.004
2. P. Drábek, P. Takáč, New patterns of travelling waves in the generalized Fisher-Kolmogorov equation, *Nonlinear Differ. Equ. Appl.*, **23** (2016). https://doi.org/10.1007/s00030-016-0365-2
3. S. Liu, R. Z. Zhang, Q. Y. Wang, X. Y. He, Sliding mode synchronization between uncertain Watts-Strogatz small-world spatiotemporal networks, *Appl. Math. Mech.-Engl.Ed.*, **41** (2020), 1833–1846. https://doi.org/10.1007/s10483-020-2686-6
4. P. Drábek, M. Zahradníková, Traveling waves for generalized Fisher-Kolmogorov equation with discontinuous density dependent diffusion, *Math. Method. Appl. Sci.*, **46** (2023), 12064–12086. https://doi.org/10.1002/mma.8683
5. G. Z. Zhu, Experiments on director waves in nematic liquid crystals, *Phys. Rev. Lett.*, **49** (1982), 1332. https://doi.org/10.1103/PhysRevLett.49.1332
6. Z. Zhang, Z. R. Zou, E. Kuhl, G. E. Karniadakis, Discovering a reaction-diffusion model for Alzheimer's disease by combining PINNs with symbolic regression, *Comput. Method. Appl. Mech. Eng.*, **419** (2024), 116647. https://doi.org/10.1016/j.cma.2023.116647
7. A. Viguerie, M. Grave, G. F. Barros, G. Lorenzo, A. Reali, A. L. G. A. Coutinho, Data-Driven simulation of Fisher-Kolmogorov tumor growth models using dynamic mode decomposition, *J Biomech. Eng.*, **144** (2022), 121001. https://doi.org/10.1115/1.4054925
8. A. Başhan, Y. Ucar, N. M. Yağmurlu, A. Esen, Numerical solutions for the fourth order extended Fisher-Kolmogorov equation with high accuracy by differential quadrature method, *Sigma J. Eng. Nat. Sci.*, **9** (2018), 273–284.

9. A. Melaibari, S. A. Mohamed, A. E. Assie, R. A. Shanab, M. A. Eltaher, Static response of 2D FG porous plates resting on elastic foundation using midplane and neutral surfaces with movable constraints, *Mathematics*, **10** (2022), 4784. https://doi.org/10.3390/math10244784
10. R. C. Mittal, S. Dahiya, A study of quintic B-spline based differential quadrature method for a class of semi-linear Fisher-Kolmogorov equations, *Alex. Eng. J.*, **55** (2016), 2893–2899. https://doi.org/10.1016/j.aej.2016.06.019
11. R. C. Mittal, G. Arora, Quintic B-spline collocation method for numerical solution of the extended Fisher-Kolmogorov equation, *Int. J. Appl. Math Mech.*, **6** (2010), 74–85.
12. R. Noureen, M. N. Naeem, D. Baleanu, P. O. Mohammed, M. Y. Almusawa, Application of trigonometric B-spline functions for solving Caputo time fractional gas dynamics equation, *AIMS Math.*, **8** (2023), 25343–25370. https://doi.org/10.3934/math.20231293
13. M. Vivas-Cortez, M. J. Huntul, M. Khalid, M. Shafiq, M. Abbas, M. K. Iqbal, Application of an extended cubic B-Spline to find the numerical solution of the generalized nonlinear time-fractional Klein-Gordon equation in mathematical physics, *Computation*, **12** (2024), 80. https://doi.org/10.3390/computation12040080
14. M. P. Alam, D. Kumar, A. Khan, Trigonometric quintic B-spline collocation method for singularly perturbed turning point boundary value problems, *Int. J. Comput. Math.*, **98** (2021), 1029–1048. https://doi.org/10.1080/00207160.2020.1802016
15. B. Karaagac, A. Esen, K. M. Owolabi, E. Pindza, A trigonometric quintic B-Spline basis collocation method for the KdV-Kawahara equation, *Numer. Analys. Appl.*, **16** (2023), 216–228. https://doi.org/10.1134/S1995423923030035
16. Y. Uçar, N. M. Yağmurlu, M. K. Yiğit, Numerical solution of the coupled Burgers equation by trigonometric B-spline collocation method, *Math. Meth. Appl. Sci.*, **46** (2023), 6025–6041. https://doi.org/10.22541/au.163257144.44242309/v1
17. L. J. T. Doss, N. Kousalya, A finite pointset method for extended Fisher-Kolmogorov equation based on mixed formulation, *Int. J. Comput. Meth.*, **18** (2021), 2050019. https://doi.org/10.1142/S021987622050019X
18. S. Kumar, R. Jiwari, R. C. Mittal, Radial basis functions based meshfree schemes for the simulation of non-linear extended Fisher-Kolmogorov model, *Wave Motion*, **109** (2022), 102863. https://doi.org/10.1016/j.wavemoti.2021.102863
19. J. Lin, Y. T. Xu, S. Reutskiy, J. Lu, A novel Fourier-based meshless method for (3+1)-dimensional fractional partial differential equation with general time-dependent boundary conditions, *Appl. Math. Lett.*, **135** (2023), 108441. https://doi.org/10.1016/j.aml.2022.108441
20. Y. H. Zhang, J. Lin, S. Reutskiy, A novel Gaussian-cubic-based backward substitution method using symmetric variable shape parameter, *Eng. Anal. Bound. Elem.*, **155** (2023), 1069–1081. https://doi.org/10.1016/j.enganabound.2023.07.026
21. M. Abbaszadeh, M. Dehghan, A. Khodadadian, C. Heitzinger, Error analysis of interpolating element free Galerkin method to solve non-linear extended Fisher-Kolmogorov equation, *Comput. Math. Appl.*, **80** (2020), 247–262. https://doi.org/10.1016/j.camwa.2020.03.014
22. N. H. Sweilam, D. M. ElSakout, M. M. Muttardi, Numerical solution for stochastic extended Fisher-Kolmogorov equation, *Chaos Soliton. Fract.*, **151** (2021), 111213. https://doi.org/10.1016/j.chaos.2021.111213

23. K. S. Nisar, S. A. M. Alsallami, M. Inc, M. S. Iqbal, M. Z. Baber, M. A.Tarar, On the exact solutions of nonlinear extended Fisher-Kolmogorov equation by using the He's variational approach, *AIMS Math.*, **7** (2022), 13874–13886. https://doi.org/10.3934/math.2022766
24. P. Danumjaya, A. K. Pani, Orthogonal cubic spline collocation method for the extended Fisher-Kolmogorov equation, *Comput. Appl. Math.*, **174** (2005), 101–117. https://doi.org/10.1016/j.cam.2004.04.002
25. L. J. T. Doss, A. P. Nandini, An H^1-Galerkin mixed finite element method for the extended Fisher-Kolmogorov equation, *Int. J. Numer. Anal. Model. Ser. B*, **3** (2012), 460–485.
26. P. Danumjaya, A. K. Pani, Numerical methods for the extended Fisher-Kolmogorov (EFK) equation, *Int. J. Numer. Anal. Mod.*, **3** (2006), 186–210.
27. H. Luo, Global attractor of the extended Fisher-Kolmogorov equation in H^k spaces, *Bound. Value Probl.*, **2011** (2011), 1–10. https://doi.org/10.1186/1687-2770-2011-39
28. N. Khiari, K. Omrani, Finite difference discretization of the extended Fisher-Kolmogorov equation in two dimensions, *Comput. Math. Appl.,* **62** (2011), 4151–4160. https://doi.org/10.1016/j.camwa.2011.09.065
29. T. Kadri, K. Omrani, A second-order accurate difference scheme for an extended Fisher-Kolmogorov equation, *Comput. Math. Appl.,* **61** (2011), 451–459. https://doi.org/10.1016/j.camwa.2010.11.022
30. A. Başhan, Quartic B-spline differential quadrature method for solving the extended Fisher-Kolmogorov equation, *Erzincan Univ. J. Sci. Tech.*, **12** (2019), 56–62.
31. B. R. Ju, W. Z. Qu, Three-dimensional application of the meshless generalized finite difference method for solving the extended Fisher-Kolmogorov equation, *Appl. Math. Lett.*, **136** (2023), 108458. https://doi.org/10.1016/j.aml.2022.108458
32. W. X. Sun, H. D. Ma, W. Z. Qu, A hybrid numerical method for non-linear transient heat conduction problems with temperature-dependent thermal conductivity, *Appl. Math. Lett.*, **148** (2024), 108868. https://doi.org/10.1016/j.aml.2023.108868
33. R. M. Hornreich, M. Luban, S. Shtrikman, Critical Behavior at the Onset of $\vec{\mathrm{k}}$-Space Instability on the λ Line, *Phys. Rev. Lett.*, **35** (1975), 1678.
34. S. G. Rubin, R. A. G. Jr, A cubic spline approximation for problems in fluid mechanics, *Tech. Rep.*, 1975.
35. N. Dhiman, M. Tamsir, A collocation technique based on modified form of trigonometric cubic B-spline basis functions for Fisher's reaction-diffusion equation, *Multidiscip. Model. Ma.*, **14** (2018), 923–939. https://doi.org/10.1108/MMMS-12-2017-0150
36. J. C. Strikwerda, *Finite difference schemes and partial differential equations*, Society for Industrial and Applied Mathematic, 2004.